BJR

Received: 2 October 2015 | Revised: 24 November 2015 | Accepted: 14 December 2015

doi: 10.1259/bjr.20150810

Cite this article as:
Murphy DJ, Lavelle LP, Gibney B, O'Donohoe RL, Rémy-Jardin M, Dodd JD. Diagnostic accuracy of standard axial 64-slice chest CT compared to cardiac MRI for the detection of cardiomyopathies. *Br J Radiol* 2016; **89**: 20150810.

FULL PAPER

Diagnostic accuracy of standard axial 64-slice chest CT compared to cardiac MRI for the detection of cardiomyopathies

[1]DAVID J MURPHY, FFRRCSI, FRCR, [1]LISA P LAVELLE, MRCPI, FFRRCSI, [1]BRIAN GIBNEY MB BCh BAO, MRCSI, [1]RORY L O'DONOHOE, MRCPI, FFRRCSI, [2]MARTINE RÉMY-JARDIN, MD and [1]JONATHAN D DODD, MRCPI, FFRRCSI

[1]Department of Radiology, St Vincent's University Hospital, Dublin, Ireland
[2]Department of Thoracic Imaging, Hospital Calmette, University Lille, CHU Lille, Lille, France

Address correspondence to: Dr David J Murphy
E-mail: *murphy.84@gmail.com*

Objective: To assess the diagnostic accuracy of standard axial chest CT compared with cardiac MRI for cardiomyopathies.

Methods: The standard axial 64-slice chest CTs of 49 patients with cardiomyopathies and 27 controls were blindly assessed for the presence of a cardiomyopathy by two independent readers. Qualitative and quantitative analysis included assessment of: (i) interatrial septal thickness, (ii) left atrial diameter, (iii) myocardial hypertrophy, thinning or fat, (iv) myocardial and papillary muscle calcification, (v) papillary muscle thickness, (vi) calcified coronary artery segments, (vii) left ventricular (LV) diameter, (viii) interventricular septal thickness and (ix) right ventricular diameters. Cardiac MRI was the gold standard.

Results: There were 21 (42.9%) dilated, 16 (32.7%) hypertrophic, 8 (16.3%) ischaemic and 4 other (8.2%) (LV non-compaction × 2, amyloid, idiopathic restrictive) patients with cardiomyopathies. An LV diameter of 47 mm, interventricular septal thickness of 14 mm and coronary artery/papillary muscle calcification on axial chest CT best distinguished dilated, hypertrophic and ischaemic cardiomyopathies from controls, respectively; kappa = 0.45 (moderate interobserver agreement). The sensitivity (95% confidence interval), specificity, positive- and negative-predictive values (95% confidence interval) and diagnostic accuracy of chest CT in diagnosing cardiomyopathies were 68% (52–83), 100%, 100%, 66% (55–85) and 80%, respectively.

Conclusion: Cardiomyopathies may be detected on standard chest CT with good sensitivity and high specificity.

Advances in knowledge: It is useful to assess for an underlying cardiomyopathy on standard chest CT, especially in a patient with unexplained dyspnoea.

INTRODUCTION

Cardiomyopathies are a heterogeneous, important group of diseases with a significant morbidity and mortality.[1] They may be classified into five major subtypes based on morphology (hypertrophic, dilated, restrictive, arrthymogenic and unclassified).[2] Such classifications assist in predicting complications and informing treatment decisions for each group. The accurate diagnosis of cardiomyopathies is based on a composite of clinical history, physical examination, laboratory tests, electrocardiography (ECG) and cardiac imaging.[3,4] Despite advances in drug therapy, the prognosis of patients with cardiomyopathies remains poor.[5] Early detection is important to ensure patients receive appropriate therapy.[6,7]

Echocardiography is generally the first imaging investigation of choice because it is accurate, safe, widely available and relatively cost effective.[8] Cardiac MRI (CMR) is now considered the imaging gold standard for evaluating cardiac structure and function but is less widely available and more expensive.[9] Its added ability to detect post-contrast myocardial fibrosis and infarction increases its utility in providing both the diagnosis of and prognosis in cardiomyopathies.[10,11]

Chest CT is one of the most widely used imaging tests for the evaluation of respiratory diseases. Traditionally, its use in evaluating cardiac disease such as cardiomyopathies has been limited by cardiac motion artefact. However, the temporal and spatial resolution of 64-slice chest CT has improved considerably, such that standard non-ECG-gated axial chest CT may allow visualization of cardiac structures with minimal motion artefact. Anecdotally, we have noted that many cardiomyopathies may be identified on standard axial 64-slice chest CT images. If standard axial chest CT allowed the detection of cardiomyopathies, it would have important clinical and prognostic implications for patients.

The aim of this study was to evaluate the diagnostic accuracy of standard axial 64-slice chest CT for the detection of cardiomyopathies compared with the gold standard of CMR.

METHODS AND MATERIALS

Patients

This single-centre retrospective study was approved by the institutional review board of St. Vincent's University Hospital. Written informed consent was waived. A retrospective search was performed of all patients at our institution who had undergone a CMR and chest CT within 12 months of each other between 2006 and 2014. A total of 50 patients (31 males and 29 females, mean age 66.4 ± 13.0 years; range 33–90 years) fulfilled these criteria. Patients referred for CMR were undergoing investigation for cardiomyopathies. Patients referred for chest CT were undergoing investigation for a variety of disorders including pulmonary embolism, emphysema, pneumonia or nodule follow-up. Exclusion criteria included cardiomyopathies relying on purely functional rather than structural criteria, such as Takotsubo cardiomyopathies, which would not be evaluable on chest CT. We included non-contrast chest CT scans because we wanted to see if there were any non-contrast CT appearances that allowed any cardiomyopathies to be identified. A group of 26 subjects (10 males and 16 females, mean age 58.5 ± 17.1 years; range 23–86 years), with normal CMRs and chest CT scans, were used as controls (Table 1).

CT protocol

All chest CT images were acquired on a 64-slice single-source CT system (Siemens Somatom® Sensation 64; Siemens Medical Solutions, Forchheim, Germany). We included a variety of chest CT protocols including CT pulmonary angiography (CTPA), standard arterial phase chest CT and high-resolution non-contrast chest CT. Slice thickness was 1–3 mm, slice interval was 0.5–1.5 mm, peak kilovoltage was 120 kVp and milliampere was 100–350 mA. Gantry rotation was 330 ms. Where contrast was given, a volume of 50–70 ml of iohexol 350 mg ml^{-1} (Omnipaque™; GE Healthcare, Little Chalfont, UK) was injected using an infusion pump at a rate of 3–4 ml s^{-1}, followed by a saline chaser (20 ml). All scans were breath-hold inspiration scans. All chest CTs were performed without ECG gating.

Table 1. Patient demographics

Demographic	Controls	All cardiomyopathies
Number	27	49
Age (years)	58.5 ± 17.1	66.4 ± 13.0
Gender	10 M/17 F	31 M/18 F
Type	–	Idiopathic dilated [21]
		Hypertrophic [16]
		Ischaemic [8]
		Other [4]

F, female; M, male.
Results are given as mean ± standard deviation.

Cardiac MRI protocol

All subjects were examined on a 1.5-T magnet (Avanto; Siemens, Erlangen, Germany) using an eight-element phased-array cardiac coil for signal reception. Left and right ventricular function was obtained with single-slice cine images using a steady-state free-precession technique [repetition time (TR), 3.5 ms; echo time (TE), 1.4 ms; matrix, 192 × 192; field of view, 34 × 34 cm; slice thickness, 6 mm; and slice gap 1 mm] obtained in two-chamber, four-chamber and short-axis planes to include the entire ventricle from the base to apex. These were followed by a bolus injection of 0.2 mmol kg^{-1} of hand-injected gadopentetate dimeglumine (Gd-DTPA; Schering AG, Berlin, Germany). Late gadolinium enhancement CMR images were obtained using single-slice double inversion-recovery-prepared gated fast gradient-echo pulse sequences, acquired approximately 10–12 minutes post-gadolinium administration. Late-enhancement images were acquired to optimally show normal myocardium/trabeculae (dark) and regions of LE within the myocardium (bright) with proper selection of the inversion time. Imaging parameters were as follows: TR 7.1 ms; TE 3.1 ms; image matrix 256 × 192; flip angle 20°; inversion pulse 180°; slice thickness 7 mm; slice gap 1 mm; and inversion time between 150 and 300 ms.

Image analysis

All chest CTs were read in a random order by one cardiac and one general radiologist (JDD, DJM, respectively) blinded to all clinical information for all image analysis. Chest CTs were read independent of CMRs. For all chest CT measurements, only standard axial images were analysed. We emphasize that our focus was on the initial qualitative detection of cardiomyopathies on standard axial chest CT.

Qualitative measurements for ischaemic cardiomyopathy included myocardial wall or papillary muscle calcification and/or myocardial wall thinning, myocardial adiposity, ventricular aneurysms and pseudo-aneurysms; hypertrophic cardiomyopathy included asymmetric myocardial wall hypertrophy; dilated cardiomyopathy included left ventricular (LV) chamber dilation significantly larger than the right ventricle chamber. Quantitative measurements included (i) interatrial septal thickness measured halfway between the mitral annulus and the lateral left atrial (LA) wall, (ii) LA long-axis diameter measured from the mitral annulus to the lateral LA wall, (iii) LV short-axis diameter measured at the level of the anteromedial papillary muscle belly, (iv) anteromedial papillary muscle belly thickness, (v) interventricular septal thickness measured at the level of the anteromedial papillary muscle belly, (vii) lateral LV wall thickness measured at the level of the anteromedial papillary muscle belly and (viii) right ventricular (RV) length and width measured from the tricuspid annulus to the RV apex and from the interventricular septum to the RV free wall, respectively. Quantitative measurements and techniques were referenced against standard published normal values (Table 2).[12–16]

A confidence score for the presence of cardiomyopathy was given for each chest CT on a four-point scale (0 = unconfident, 1 = low confidence, 2 = moderate confidence and 3 = high

Table 2. Diagnostic accuracy of standard axial chest CT for cardiomyopathies

Cardiomyopathies	Sensitivity	Specificity	PPV	NPV	+LR	−LR	DA
Controls	1.0	1.0	1.0	1.0	–	–	1.0
Dilated	0.48 (0.26–0.69)	1.0	1.0	0.69	>10	0.52	0.76
Hypertrophic	0.88 (0.73–1.0)	1.0	1.0	0.93	>10	0.11	0.95
Ischaemic	0.50 (0.15–0.85)	1.0	1.0	0.86	>10	0.5	0.88
All	0.68 (0.52–0.83)	1.0	1.0	0.66	>10	0.33	0.80

DA, diagnostic accuracy; LR, likelihood ratio; NPV, negative-predictive value; PPV, positive-predictive value.
Results are mean (95% confidence interval).

confidence). Each chest CT was also scored on a four-point scale for cardiac motion artefact (0 = severe cardiac motion precluding a diagnosis, 1 = moderate, 2 = mild and 3 = none).

Each quantitative measurement was then repeated on the CMR scans, independent and blinded to the CT analysis. The diagnosis of cardiomyopathy on MRI was based on contemporary standard cardiomyopathy diagnostic criteria.[2,17–20]

Statistical analysis

Continuous variables are presented as mean ± standard deviation. Categorical variables are presented as frequencies and percentages. Group comparison of continuous variables was performed by Student's independent *t* test. Group comparisons of categorical variables were performed by Fisher's exact test. Correlations were performed using Spearman's rank test. Interobserver agreement was assessed using kappa analysis. Receiver-operator curve analysis was used to assess cut-off values for quantitative measurements of each cardiomyopathy. All statistical analyses were performed with SPSS v. 12.0 (IBM Corp., New York, NY; formerly SPSS Inc., Chicago, IL). All statistical tests were two sided, and a value of $p < 0.05$ was considered significant.

RESULTS

There were 50 patients with cardiomyopathies and 27 controls in the initial cohort. One cardiomyopathy was excluded owing to purely functional, non-structural abnormalities in a patient with Takotsubo cardiomyopathy (which would be undetectable on standard chest CT), leaving 49 cardiomyopathies in the final analysis. Patient demographics are shown in Table 1. Significant differences between control and cardiomyopathy groups were noted in age (58.5 ± 17.1 *vs* 66.4 ± 13.0 years, $p < 0.05$) and gender (10 *vs* 31 males, $p < 0.05$). Of the cardiomyopathies, there were 21 (42.9%) dilated (DCM) (Figure 1; Supplementary Figure 1), 16 (32.7%) hypertrophic (HCM) (Figure 2; Supplementary Figure 2), 8 (16.3%) ischaemic (Figure 3) and 4 (8.2%) other cardiomyopathies [2 (4.1%) LV non-compaction, 1 (2%) amyloid and 1 (2%) idiopathic restrictive cardiomyopathy] (Figure 4). Our hypotrophic subset included a patient with apical variant hypertrophic cardiomyopathy (Figure 4). There were four non-contrast chest CT scans in the control group and one non-contrast chest CT scan in the cardiomyopathies group. Figure 5 illustrates normal measurements on chest CT from one of the controls.

Overall sensitivity (95% confidence interval), specificity, positive- and negative-predictive values (95% confidence interval) and diagnostic accuracy for all cardiomyopathies were 68% (52–83), 100%, 100%, 66% (55–85) and 80%, respectively (Table 2). Of the false-negative cases, nine cases were DCM, two cases were ischaemic, one case was HCM, one case was cardiac amyloid and one case was restrictive cardiomyopathy. Of the nine false-negative DCM cardiomyopathies, mean LV diameter was 60.7 mm, indicating a mild level of severity (maximum LV diameter was 85 mm). Of the two false-negative ischaemic

Figure 1. A 67-year-old male with shortness of breath. (a) Standard chest CT demonstrated normal lungs and a severely dilated left ventricle (arrow, end-diastolic diameter = 77 mm). (b) Corresponding cardiac MRI (CMR) confirms a severely dilated left ventricle (arrow, end-diastolic diameter = 85 mm) consistent with a dilated cardiomyopathy.

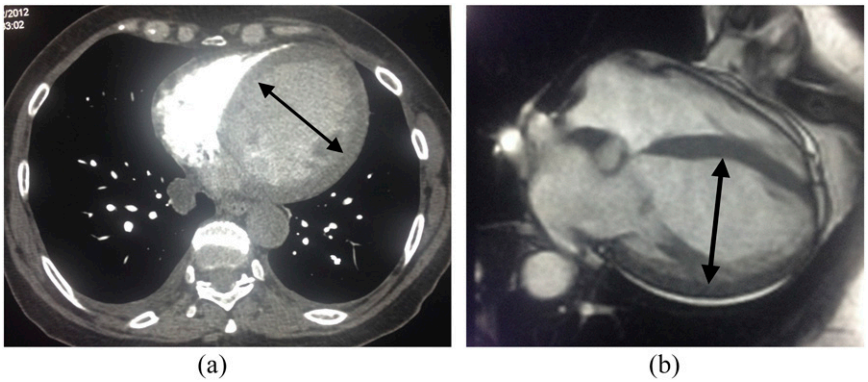

(a) (b)

Figure 2. A 77-year-old female with shortness of breath and palpitations. (a) Standard axial chest CT demonstrated normal lungs and asymmetric hypertrophy of the interventricular septum (arrow, 32 mm). (b) Corresponding cardiac MRI (CMR) confirms asymmetric hypertrophy of the interventricular septum (arrow, 25 mm) consistent with a hypertrophic cardiomyopathy.

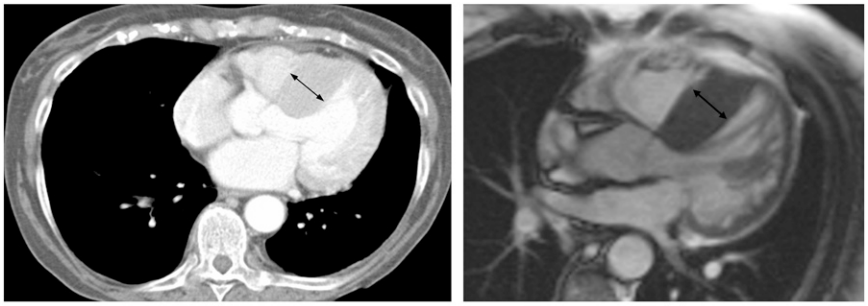

(a) (b)

cardiomyopathies, one CT was a CTPA with low contrast density in the LV and one CT was a non-contrast scan. The single false-negative HCM case was also a CTPA with low contrast density in the LV. Hypertrophic cardiomyopathies were identified with the highest diagnostic accuracy (97%) followed by ischaemic (89%) and dilated (81%) cardiomyopathies (Table 2). Kappa analysis between the two radiologists for the diagnosis of cardiomyopathies on chest CT was 0.45, indicating moderate interobserver agreement.

Correlations and comparisons between the two groups are detailed in Tables 3 and 4 and Figure 6. Significant differences were seen between controls and patients with cardiomyopathies on standard axial chest CT in LA diameter (34.4 ± 6.9 *vs* 44.2 ± 9.6 mm, $p < 0.01$), LV diameter (42.5 ± 6.1 *vs* 52.9 ± 11.5 mm, $p < 0.001$), papillary muscle calcification (0.0 *vs* 4.0, $p < 0.001$), interventricular septal thickness (8.0 ± 2.2 *vs* 12.3 ± 7.3 mm, $p < 0.01$), lateral wall thickness (6.4 ± 1.7 *vs* 7.8 ± 2.9 mm, $p < 0.05$), myocardial wall thinning (0.0 *vs* 1.0), myocardial calcification (0.0 *vs* 2.0), coronary artery calcification (1.0 ± 2.0 *vs* 3.4 ± 4.3) and RV long axis (51.9 ± 8.4 *vs* 61.8 ± 12.6, $p = 0.01$) (Table 3). Papillary muscle thickness was not significantly different between the two groups, but when a subanalysis of controls *vs* patients with HCM was performed, significantly smaller papillary muscles were detected in the control group *vs* the HCM group (7.1 ± 2.0 *vs* 11.3 ± 2.9, $p < 0.0001$) (Figure 6).

Ischaemic cardiomyopathies were the most confidently diagnosed cardiomyopathy on standard axial chest CT (75%), followed by hypertrophic cardiomyopathy (66.7%) then dilated cardiomyopathy (38%) (Figure 7). All controls were identified correctly on chest CT. Regarding cardiac motion artefact scores, 7 chest CT scans were scored as severe, 6 scans as moderate, 34 scans as mild and 27 scans as no cardiac motion artefact.

Receiver-operator curve analysis of LV diameter for the diagnosis of DCM showed an area under the curve of 0.92 with a cut-off LV diameter of 47 mm giving a sensitivity of 93% and specificity of 88%, $p < 0.0001$ (Figure 8). Receiver-operator curve analysis of interventricular septal thickness for the diagnosis of HCM showed an area under the curve of 0.95 with a cut-off LV interventricular septum thickness of 14 mm giving a sensitivity of 83% and specificity of 100%, $p < 0.0001$ (Figure 8). Receiver-operator curve analysis of papillary muscle thickness for the diagnosis of HCM showed an area under the curve of 0.95 with a cut-off LV interventricular septum thickness of 9 mm giving a sensitivity of 100% and specificity of 94%, $p < 0.0001$ (Figure 8).

Figure 3. A 77-year-old male with shortness of breath. (a) Standard axial non-contrast chest CT demonstrated normal lungs and a calcified papillary muscle (arrow) consistent with papillary muscle infarction. Note also the right coronary artery calcified plaque. (b) Corresponding cardiac MRI confirms late gadolinium enhancement of the left-ventricular mid-level inferolateral segment (arrow) consistent with a chronic myocardial infarction.

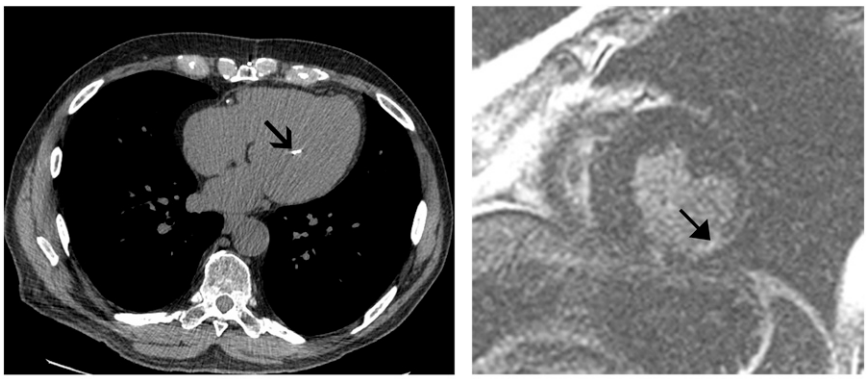

(a) (b)

Figure 4. A 59-year-old female with shortness of breath. (a) Standard axial non-contrast chest CT demonstrated normal lungs and severe apical myocardial segment hypertrophy (arrow) suggesting apical variant hypertrophic cardiomyopathy (HCM). (b) Corresponding cardiac MRI (CMR) confirms apical variant HCM (arrow). Note the complete obliteration of the ventricular chamber lumen at the apex on both CT and CMR.

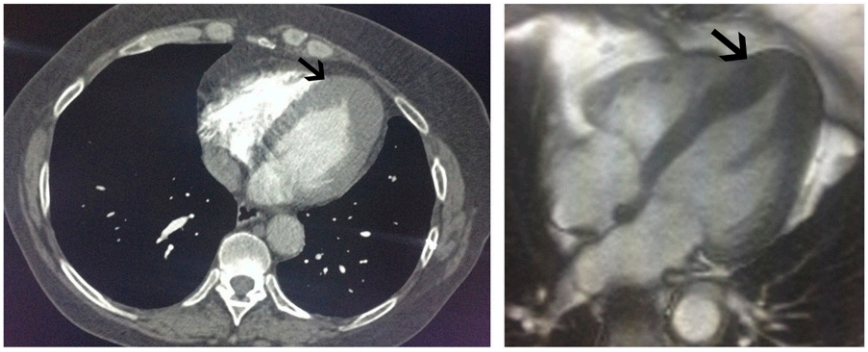

(a) (b)

DISCUSSION

This study demonstrated that cardiomyopathies can be identified on standard axial chest CT with good sensitivity and high specificity compared with the gold standard of CMR. To our knowledge, we are the first to show that standard axial chest CT can detect a variety of cardiomyopathies with good diagnostic accuracy. We emphasize that our focus in this study was on the initial detection. We did not attempt to use double-oblique cardiac imaging planes on chest CT since most chest radiologists do not perform these in routine practice. We do routinely perform sagittal and coronal CT reformats, but we have anecdotally attempted to use these for diagnosing cardiomyopathies and found them challenging to interpret. In practice, if we suspect a cardiomyopathy on standard axial chest CT, we perform dedicated cardiac imaging plane analysis thereafter, but it is the initial detection that is the key. We also emphasize that this was not a prevalence study, and the ratio of cardiomyopathy to normal cases in this cohort is likely to be artificially high compared with everyday practice.

We found dilated LV diameters, interventricular septal/papillary muscle hypertrophy and coronary and papillary muscle calcification to be the most useful features in detecting and differentiating between dilated, hypertrophic and ischaemic cardiomyopathies, respectively. We did not find RV dimensions useful, although we did detect significant differences between controls and patients with cardiomyopathies for this parameter. The RV is more variable in size and shape than the LV under normal and pathological conditions, and this was reflected in the wider standard deviations in our cohort in both control and cardiomyopathy groups. All patients with ischaemic cardiomyopathies had at least one

Table 3. Normal reference values, study measurements and correlations between standard axial chest CT and cardiac MRI for cardiomyopathies

Quantitative	Normal reference values	Chest CT	Cardiac MRI	*R*-value
Coronary artery calcification	–	26	0	–
PM calcification	–	3	0	–
Myocardial wall thinning	–	1	7	–
Myocardial calcification	–	2	0	–
Qualitative				
IAS (mm)	2.0	2.5 (1.8)	3.2 (1.4)	0.53[b]
LA (cm)	2.2–4.2	43.3 (11.7)	41.3 (10.5)	0.51[b]
LV diameter (mm)	39–53	48.6 (11.2)	56.1 (10.5)	0.77[b]
IVS (mm)	6–9	10.8 (5.9)	10.2 (4.8)	0.81[b]
Lateral wall thickness (mm)	6–9	7.2 (2.4)	7.2 (2.1)	0.71[a]
PM thickness (mm)	3–5	8.3 (3.5)	7.3 (2.4)	0.41[b]
RV long axis (mm)	71–79	61.8 (12.6)	66.9 (13.9)	0.66[b]
RV short axis (mm)	27–33	30.7 (8.2)	30.0 (7.2)	0.51[b]

IAS, interatrial septum; IVS, interventricular septum; LA, left atrial; LV, left ventricular; PM, papillary muscle; RV, right ventricular.
[a]$p < 0.05$.
[b]$p < 0.01$.

Table 4. Comparison between controls and cardiomyopathies on standard axial chest CT

Measurement	Controls	Cardiomyopathies
Left atrium		
Interatrial septal thickness (mm)	2.8 (2.0)	2.2 (1.8)
Left atrium diameter (mm)	34.4 (6.9)	43.8 (8.7)[a]
Left ventricular cavity		
Diameter (mm)	42.5 (6.1)	52.9 (11.5)[b]
Papillary muscle calcification (*n*)	0.0	5.0[b]
Papillary muscle thickness (mm)	7.1 (2.0)	7.5 (2.6)
Left ventricular myocardium		
Interventricular septal thickness (mm)	8.0 (2.2)	10.8 (6.1)[a]
Lateral wall thickness (mm)	64 (1.7)	73 (2.4)[c]
Myocardial wall thinning (*n*)	0.0	1.0
Myocardial calcification (*n*)	0.0	2.0
Coronary artery calcification (*n*)	1.0 (2.0)	2.9 (4.2)[c]
RV dimensions		
RV long axis (mm)	52.9 (8.9)	60.9 (11.8)[a]
RV short axis (mm)	29.9 (6.7)	30.6 (9.4)

RV, right ventricular.
Results are given as mean (standard deviation).
[a]$p < 0.01$.
[b]$p < 0.001$.
[c]$p < 0.05$.

calcified coronary artery segment, and the combination of coronary and papillary muscle calcification increased the level of confidence in diagnosing ischaemic cardiomyopathies. Similarly, a combination of interventricular septal and papillary muscle hypertrophy together increased the level of confidence in diagnosing HCM. The pitfalls we found when

Figure 5. Standard axial non-contrast CT chest demonstrating (a) normal papillary muscle thickness (line), (b) normal interventricular septal thickness (line) and normal (c) left ventricular (crossed lines) and (d) right ventricular (crossed lines) diameters.

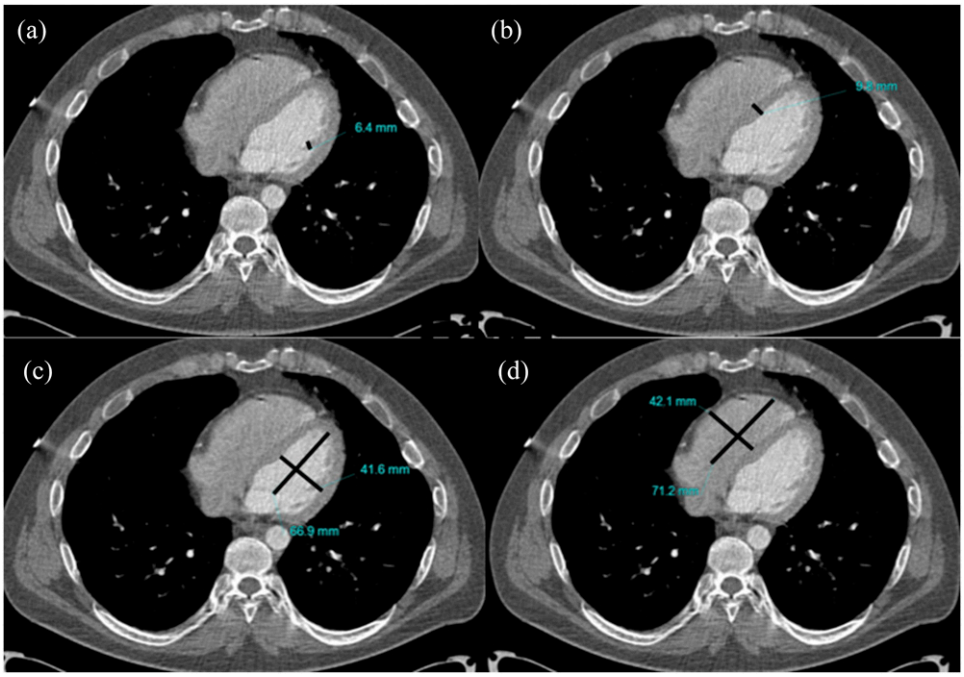

Figure 6. Individual correlations (circles) between standard axial chest CT and cardiac MRI for (a) left ventricular end-diastolic diameter ($R^2 = 0.7$, $p < 0.001$) and (b) interventricular septum thickness ($R^2 = 0.8$, $p < 0.001$). Axis measurements are in mm.

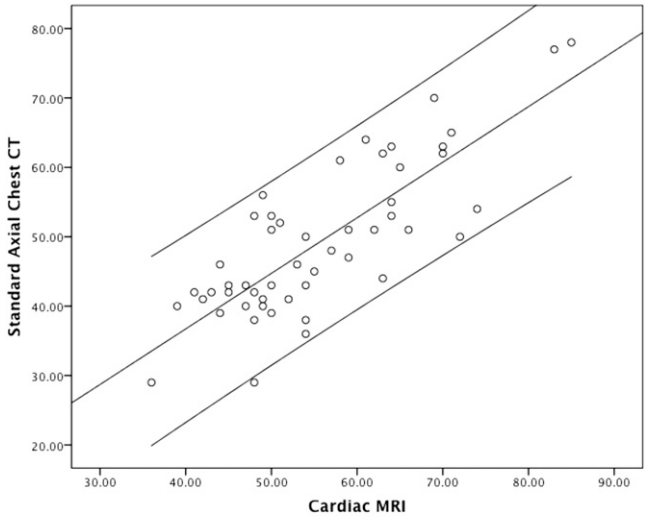

(a)

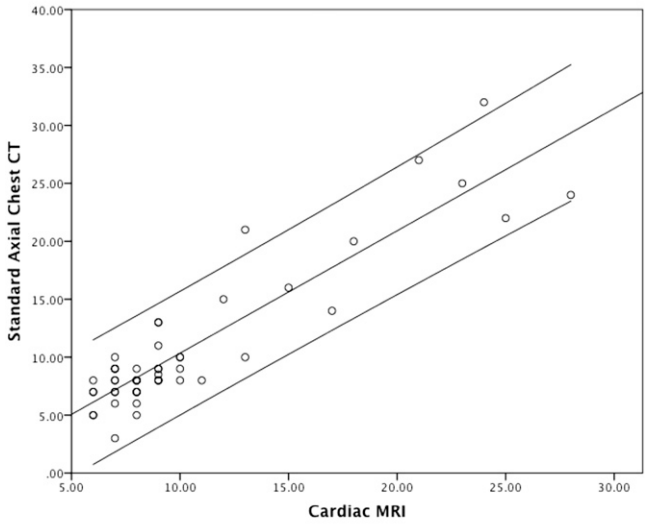

(b)

interpreting chest CT for cardiac abnormalities included structurally similar cardiomyopathies such as cardiac amyloid and HCM cases, both of which cause myocardial hypertrophy.[21]

Cardiac motion artefact resulted in 10 false-negative cases. It led to an overall underestimation of LV diameter and overestimation of interventricular septal thickness. The underestimation related to trabeculae merging with the myocardial wall, resulting in a smaller appearing ventricular cavity and thicker interventricular septa. Rapidly evolving CT technology developments are likely to reduce this limitation. Of particular note is dual-source CT, a scanner with a high temporal resolution, resulting in reduced cardiac motion artefact. Karlo et al[22] utilized second-generation high-pitch dual-source chest CT without ECG gating to assess the image quality of the aortic valve. In 120 patients, they found high diagnostic image quality for aortic valve evaluation without cardiac motion artefact. Even higher temporal resolutions of 66 ms are reported with the latest third-generation dual-source CT.[23]

The type of chest CT contrast protocol also influenced the results. Non-contrast scan followed by CTPA was the most difficult scan to analyse. Almost all chest CT scans scored as no or low confidence had none or poor contrast density in the left ventricle. This was a particular issue for CTPA, in which the timing of contrast was focused in the right rather than the left heart chambers. Thus, a consideration when performing CTPA is whether to include a triphasic contrast-infusion protocol in order to opacity both right and left heart chambers. In the context of the present study, this would likely have lead to an increased number of readable scans, albeit with the disadvantage of a slightly increased contrast volume.

Although non-contrast studies led to some false negatives, they nevertheless also yielded considerable information. Calcification in the coronary arteries or papillary muscles was an important feature in identifying ischaemic cardiomyopathies, which is easier to detect on non-contrast chest CT as well as CMR. Dutch and Italian lung cancer CT screening trials have reported the ability of non-cardiac-gated chest CT to detect coronary artery disease.[24–26] Chiles et al[27] have shown that a global assessment of the volume of calcified coronary artery plaque in smokers undergoing non-cardiac-gated chest CTs can help risk stratify patients for coronary heart disease associated mortality. However, there is no evidence that standard axial chest CT has the ability to detect cardiomyopathies *per se*, and we could not find another published series with which to compare our results too.

The implications of our findings are that in practice, if standard axial chest CT (Figure 5) shows a dilated left ventricle >47 mm, a hypertrophied interventricular septum >14 mm/papillary muscle hypertrophy >9 mm or myocardial or papillary muscle calcification, we perform dedicated cardiac imaging plane analysis thereafter. An echocardiogram is the next appropriate investigation to confirm the diagnosis and assess ventricular function, possibly followed by CMR. Treatment typically includes medical therapy with beta-blockers and angiotension converting enzyme inhibitors

Figure 7. Levels of scoring confidence for the diagnosis of cardiomyopathies on standard axial chest CT. Lines indicate confidence intervals. DCM, dilated; HCM, hypertrophic; ISCH, ischaemic.

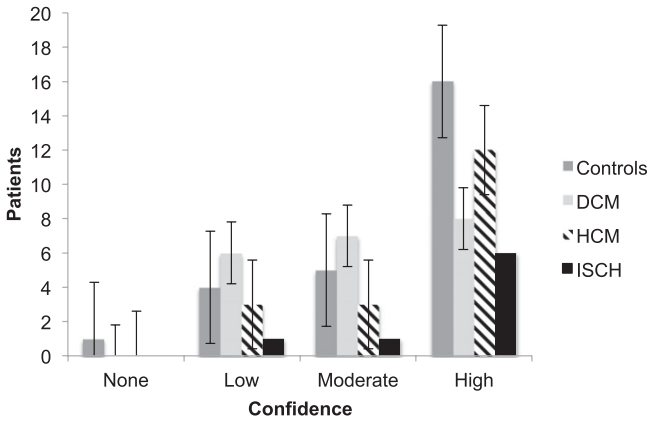

Figure 8. Receiver-operator curve analysis for (a) left ventricular diameter in dilated cardiomyopathy (DCM), (b) interventricular septal thickness in hypertrophic cardiomyopathy (HCM) and (c) papillary muscle thickness in HCM on standard axial chest CT compared with controls. (a) The area under the curve (AUC) = 0.92, $p < 0.0001$, using a cut-off value of 47 mm, yielded a sensitivity and specificity of 93% and 88%, respectively. (b) The AUC = 0.95, $p < 0.0001$, using a cut-off value of 14 mm, yielded a sensitivity and specificity = 83% and 100%, respectively. (c) The AUC = 0.95, $p < 0.0001$, using a cut-off value of 9 mm, yielded a sensitivity and specificity = 100% and 94%, respectively.

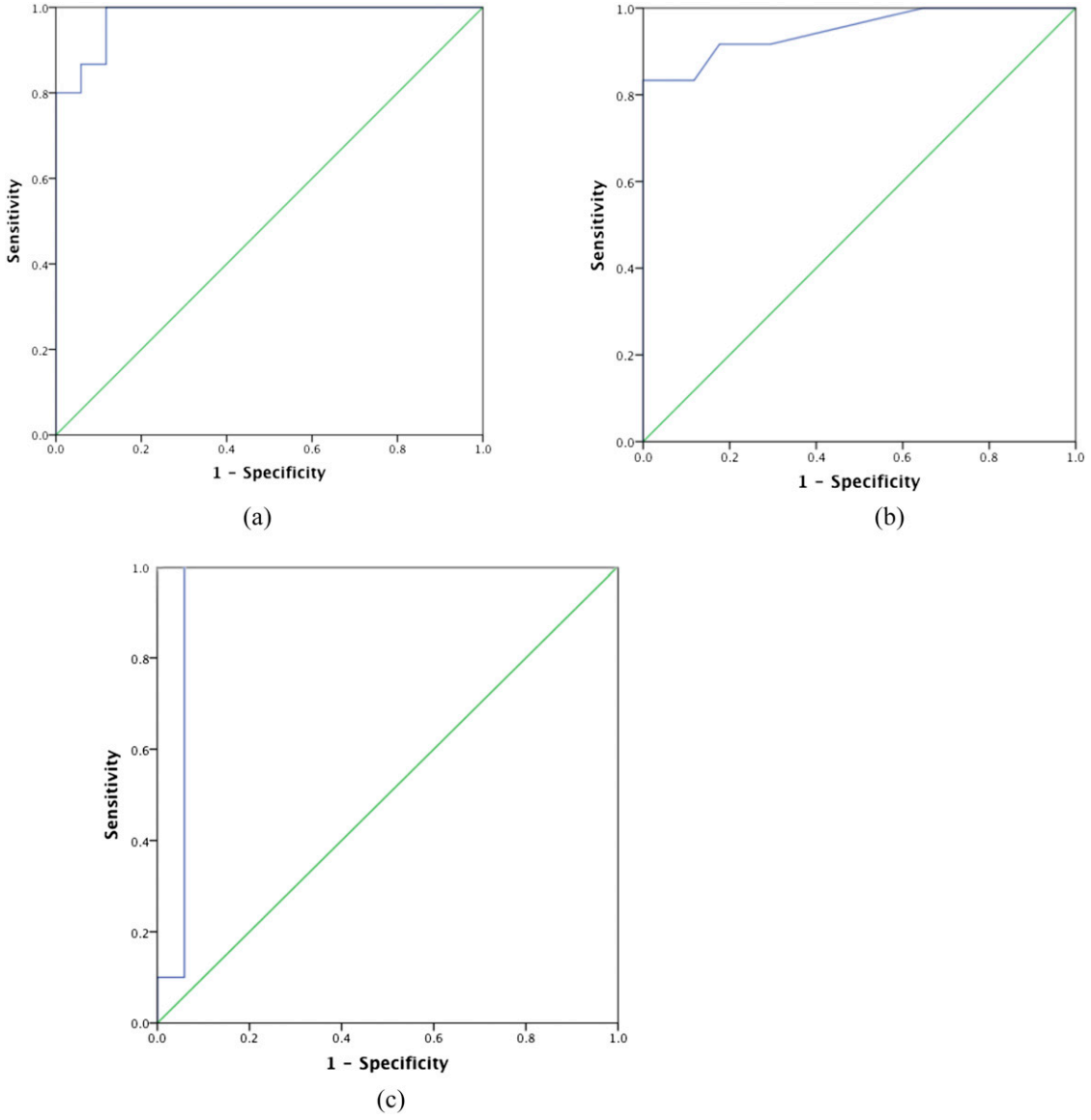

(a) (b) (c)

for dilated cardiomyopathies, beta-blockade for HCM and secondary preventative therapy for ischaemic cardiomyopathies. Consideration may also be given to implantable defibrillator therapy. Finally, screening of first-degree relatives would also be undertaken if relevant. Thus, initial detection on chest CT carries considerable implications for patients.

Our study has several limitations. The study cohort is small, but obtaining patients who had both an MRI and chest CT proved difficult, since chest CT is not commonly ordered by cardiologists. This was not a prevalence study, and the ratio of cardiomyopathy to normal cases in this cohort is likely to be much lower in everyday practice. There is some degree of reader bias, although we included as many controls as possible that had undergone both CT and MRI. Almost all the HCM cases in our cohort had hypertrophy of the interventricular septum, and it would be interesting to assess our observations in a more phenotypically variable group.

CONCLUSION

Standard axial 64-slice chest CT detects cardiomyopathies with good sensitivity and high specificity. Dilated ventricular diameters, interventricular septal/papillary muscle hypertrophy and coronary artery/papillary muscle calcification are useful specific chest CT features for dilated, hypertrophic and ischaemic cardiomyopathies, respectively.

REFERENCES

1. Maron BJ, Towbin JA, Thiene G, Antzelevitch C, Corrado D, Arnett D, et al. Contemporary definitions and classification of the cardiomyopathies: an American Heart Association scientific statement from the council on clinical cardiology, heart failure and transplantation committee; quality of care and outcomes research and functional genomics and translational biology interdisciplinary working groups; and Council on Epidemiology and Prevention. *Circulation* 2006; **113**: 1807–16. doi: 10.1161/CIRCULATIONAHA.106.174287
2. Elliott P, Andersson B, Arbustini E, Bilinska Z, Cecchi F, Charron P, et al. Classification of the cardiomyopathies: a position statement from the European Society of Cardiology Working Group on myocardial and pericardial diseases. *Eur Heart J* 2008; **29**: 270–6. doi: 10.1093/eurheartj/ehm342
3. Yancy CW, Jessup M, Bozkurt B, Butler J, Casey DR, Drazner MH, et al. 2013 ACCF/AHA guideline for the management of heart failure: executive summary: a report of the American College of Cardiology Foundation/American Heart Association Task Force on practice guidelines. *Circulation* 2013; **128**: 1810–52. doi: 10.1161/CIR.0b013e31829e8807
4. Rapezzi C, Arbustini E, Caforio ALP, Charron P, Gimeno-Blanes J, Helio T, et al. Diagnostic work-up in cardiomyopathies: bridging the gap between clinical phenotypes and final diagnosis. A position statement from the ESC Working Group on myocardial and pericardial diseases. *Eur Heart J* 2013; **34**: 1448–58. doi: 10.1093/eurheartj/ehs397
5. Felker GM, Thompson RE, Hare JM, Hruban RH, Clemetson DE, Howard DL, et al. Underlying causes and long-term survival in patients with initially unexplained cardiomyopathy. *N Engl J Med* 2000; **342**: 1077–84. doi: 10.1056/NEJM200004133421502
6. Hershberger RE, Cowan J, Morales A, Siegfried JD. Progress with genetic cardiomyopathies: screening, counseling, and testing in dilated, hypertrophic, and arrhythmogenic right ventricular dysplasia/cardiomyopathy. *Circ Heart Fail* 2009; **2**: 253–61. doi: 10.1161/CIRCHEARTFAILURE.108.817346
7. Bart BA, Shaw LK, McCants CBJ, Fortin DF, Lee KL, Califf RM, et al. Clinical determinants of mortality in patients with angiographically diagnosed ischemic or nonischemic cardiomyopathy. *J Am Coll Cardiol* 1997; **30**: 1002–8. doi: 10.1016/S0735-1097(97)00235-0
8. Douglas PS, Garcia MJ, Haines DE, Lai WW, Manning MJ, Patel AR, et al. ACCF/ASE/AHA/ASNC/HFSA/HRS/SCAI/SCCM/SCCT/SCMR 2011 appropriate use criteria for echocardiography. *J Am Soc Echocardiogr* 2011; **24**: 229–67. doi: 10.1016/j.echo.2010.12.008
9. American College of Cardiology Foundation Task Force on Expert Consensus Documents; Hundley WG, Bluemke DA, Finn JP, Flamm SD, Fogel MA, Friedrich MG, et al. ACCF/ACR/AHA/NASCI/SCMR 2010 expert consensus document on cardiovascular magnetic resonance: a report of the American college of cardiology foundation task force on expert consensus documents. *Circulation* 2010; **121**: 2462–508.
10. Kramer CM, Barkhausen J, Flamm SD, Kim RJ, Nagel E. Society for cardiovascular magnetic resonance board of trustees task force on standardized protocols. Standardized cardiovascular magnetic resonance imaging (CMR) protocols, society for cardiovascular magnetic resonance: board of trustees task force on standardized protocols. *J Cardiovasc Magn Reson* 2008; **10**: 35. doi: 10.1186/1532-429X-10-35
11. Hundley WG, Bluemke D, Bogaert JG, Friedrich MG, Higgins CB, Lawson MA, et al. Society for cardiovascular magnetic resonance guidelines for reporting cardiovascular magnetic resonance examinations. *J Cardiovasc Magn Reson* 2009; **11**: 5. doi: 10.1186/1532-429X-11-5
12. Maceira AM, Prasad SK, Khan M, Pennell DJ. Reference right ventricular systolic and diastolic function normalized to age, gender and body surface area from steady-state free precession cardiovascular magnetic resonance. *Eur Heart J* 2006; **27**: 2879–88. doi: 10.1093/eurheartj/ehl336
13. Maceira AM, Prasad SK, Khan M, Pennell DJ. Normalized left ventricular systolic and diastolic function by steady state free precession cardiovascular magnetic resonance. *J Cardiovasc Magn Reson* 2006; **8**: 417–26. doi: 10.1080/10976640600572889
14. Maceira AM, Cosín-Sales J, Roughton M, Prasad SK, Pennell DJ. Reference left atrial dimensions and volumes by steady state free precession cardiovascular magnetic resonance. *J Cardiovasc Magn Reson* 2010; **12**: 65. doi: 10.1186/1532-429X-12-65
15. Maceira AM, Cosín-Sales J, Roughton M, Prasad SK, Pennell DJ. Reference right atrial dimensions and volume estimation by steady state free precession cardiovascular magnetic resonance. *J Cardiovasc Magn Reson* 2013; **15**: 29. doi: 10.1186/1532-429X-15-29
16. Lang RM, Bierig M, Devereux RB, Flachskampf FA, Foster E, Pellikka PA, et al. Recommendations for chamber quantification: a report from the American Society of Echocardiography's Guidelines and Standards Committee and the Chamber Quantification Writing Group, developed in conjunction with the European Association of Echocardiography, a branch of the European Society of Cardiology. *J Am Soc Echocardiogr* 2005; **18**: 1440–63. doi: 10.1016/j.echo.2005.10.005
17. Moon JC, Fisher NG, McKenna WJ, Pennell DJ. Detection of apical hypertrophic cardiomyopathy by cardiovascular magnetic resonance in patients with non-diagnostic echocardiography. *Heart* 2004; **90**: 645–9. doi: 10.1136/hrt.2003.014969
18. Moon JC, McKenna WJ, McCrohon JA, Elliott PM, Smith GC, Pennell DJ. Toward clinical risk assessment in hypertrophic cardiomyopathy with gadolinium cardiovascular magnetic resonance. *J Am Coll Cardiol* 2003; **41**: 1561–7. doi: 10.1016/S0735-1097(03)00189-X
19. Assomull RG, Prasad SK, Lyne J, Smith G, Burman ED, Khan M. Cardiovascular magnetic resonance, fibrosis, and prognosis in dilated cardiomyopathy. *J Am Coll Cardiol* 2006; **48**: 1977–85. doi: 10.1016/j.jacc.2006.07.049
20. Maceira AM, Joshi J, Prasad SK, Moon JC, Perugini E, Harding I, et al. Cardiovascular magnetic resonance in cardiac amyloidosis. *Circulation* 2005; **111**: 186–93. doi: 10.1161/01.CIR.0000152819.97857.9D
21. Moon JC, Reed E, Sheppard MN, Elkington AG, Ho SY, Burke M, et al. The histologic basis of late gadolinium enhancement cardiovascular magnetic resonance in hypertrophic cardiomyopathy. *J Am Coll Cardiol* 2004; **43**: 2260–4. doi: 10.1016/j.jacc.2004.03.035
22. Karlo C, Leschka S, Goetti RP, Feuchtner G, Desbiolles L, Stolzmann P, et al. High-pitch dual-source CT angiography of the aortic valve-aortic root complex without ECG-synchronization. *Eur Radiol* 2011;

21: 205–12. doi: 10.1007/s00330-010-1907-3

23. Flohr TG, De Cecco CN, Schmidt B, Wang R, Schoepf UJ, Meinel FG. Computed tomographic assessment of coronary artery disease: state-of-the-art imaging techniques. *Radiol Clin North Am* 2015; **53**: 271–85. doi: 10.1016/j.rcl.2014.11.011
24. Church TR, Black WC, Aberle DR, Berg CD, Clingan KL, Duan F, et al. Results of initial low-dose computed tomographic screening for lung cancer. *N Engl J Med* 2013; **368**: 1980–91. doi: 10.1056/NEJMoa1209120
25. Jacobs PC, Prokop M, van der Graaf Y, Gondrie MJ, Janssen KJ, de Koning HJ, et al. Comparing coronary artery calcium and thoracic aorta calcium for prediction of all-cause mortality and cardiovascular events on low-dose non-gated computed tomography in a high-risk population of heavy smokers. *Atherosclerosis* 2010; **209**: 455–62. doi: 10.1016/j.atherosclerosis.2009.09.031
26. Mets OM, de Jong PA, Prokop M. Computed tomographic screening for lung cancer: an opportunity to evaluate other diseases. *JAMA* 2012; **308**: 1433–4. doi: 10.1001/jama.2012.12656
27. Chiles C, Duan F, Gladish GW, Ravenel JG, Baginski SG, Snyder BS, et al. Association of coronary artery calcification and mortality in the national lung screening trial: a comparison of three scoring methods. *Radiology* 2015; **276**: 82–90. doi: 10.1148/radiol.15142062